MODULUS OF ELASTICITY AND HARDNESS OF COMPRESSION AND OPPOSITE WOOD CELL WALLS OF MASSON PINE

Yanhui Huang,[a] Benhua Fei,[a,]* Yan Yu,[a] Siqun Wang,[b] Zengqian Shi,[b] and Rongjun Zhao [c]

Compression wood is commonly found in Masson pine. To evaluate the mechanical properties of the cell wall of Masson pine compression and opposite wood, nanoindentation was used. The results showed that the average values of hardness and cell wall modulus of elasticity of opposite wood were slightly higher than those of compression wood. With increasing age of the annual ring, the modulus of elasticity showed a negative correlation with microfibril angle, but a weak correlation was observed for hardness. In opposite and compression wood from the same annual ring, the differences in average values of modulus of elasticity and hardness were small. These slight differences were explained by the change of microfibril angle (MFA), the press-in mode of nanoindentation, and the special structure of compression wood. The mechanical properties were almost the same for early, transition, and late wood in a mature annual ring of opposite wood. It can therefore be inferred that the average modulus of elasticity (MOE) and hardness of the cell walls in a mature annual ring were not being affected by cell wall thickness.

Keywords: Compression wood; Cell wall; Modulus of elasticity; Hardness; Nanoindentation

Contact information: a: International Center for Bamboo and Rattan, Beijing, China, 100102; b: Center for Renewable Carbon, University of Tennessee, Knoxville, TN 37996-4570, USA; c: Research Institute of Wood Industry, Chinese Academy of Forestry, Beijing, China, 100091;
**Corresponding author: feibenhua@icbr.ac.cn*

INTRODUCTION

Compression wood develops because of the mechanical compression that occurs on the lower sides of leaning trunks and branches of gymnosperm trees. Wood from the corresponding upper side of these stems and branches is called opposite wood. The characteristics of opposite wood are similar to normal wood; that is, wood that has not grown and developed under the compressive or tensile loads associated with applied bending forces. In contrast to normal or opposite wood, the distinct characteristics of compression wood are higher lignification and density. Compression woods have a unique cell wall structure and tracheid formation characterized by the lack of an S_3 layer and helical cavities in the S_2 layer of the cell wall, rounded cross sections and distorted tracheid tips, and high microfibril angles (Timell 1987). The chemistry of tracheids in compression wood is characterized by lower contents of cellulose and higher contents of lignin compared to a tracheid in normal wood (Timell 1987).

Masson pine (*Pinus massoniana*) is an important commercial species in the south of China and is used mainly in construction, furniture, indoor decorating, and pulp and papermaking. Compression wood is commonly found in the stems and branches of plantation Masson pine. The compression wood has an important influence on the mechanical properties of wood and wood-based products because of its specific structure and chemical composition. The macro-mechanical properties of compression wood have been subjected to detailed research; however, the mechanical properties at the cellular and subcellular level of compression wood are not well reported. Burgert *et al.* (2004) measured the longitudinal mechanical properties of single fibers of four compression wood types at the cellular level. Gindl *et al.* (2004) and Konnerth *et al.* (2009) investigated the relationship between cell wall mechanical properties of tracheids and microfibril angle (MFA) with normal, early, and late wood, as well as compression and opposite wood at the subcellular level by using a nano-indentation technique. For compression and opposite wood, there has been no detailed and systematic examination of the influence of MFA on the mechanical properties of the cell wall S_2 layer of tracheids, especially looking at the mechanical properties within an annual ring.

To better understand the mechanical properties of the cell wall S_2 layer of compression and opposite wood, this research aims to discuss systematically the influence of microfibril angle (MFA) on the longitudinal modulus of elasticity (MOE) and hardness of compression and opposite wood of Masson pine. The mechanical properties of the cell wall S_2 layer of opposite wood within an annual ring are also examined and discussed.

MATERIALS AND METHODS

The experimental Masson pine was 32-years-old, growing in the Huangshan Gongyi Forest Farm in Anhui province. A 4-cm-thick disk containing compression and opposite wood was taken from the Masson pine crooked trunk at a height of 1.5 m. The disk was then dried in air for one month. After drying, one 10-mm-wide center strip was sawn from the disk, and six slices containing latewood from the 2nd, 4th, 6th, 9th, 15th, and 24th annual rings (counted from the pith) were removed from the strip on the compression and opposite sides. The nominal size of the slices was about 40×1×10 mm (longitudinal × radial × tangential).

All the slices were conditioned at 20 °C and 60% relative humidity for a week before measuring the microfibril angle using X-ray diffraction (X'PERTPRO, Philips Analytical, Almelo, Holland). The radiation source was CuKa (λ=0.154 nm). The tube voltage and current were 40 KV and 40 mA, respectively. The X-ray beam size was 4 by 2 mm, and the scattering angle 2θ was 22.4°. The scan time of each sample was 3 minutes. The results were analyzed to extract diffraction strength curves and calculate the mean microfibril angle (MFA). The MFA was determined using the method developed by Cave (1966).

The 12 slices were cut to the final dimensions of 1 mm in the radial direction, 1 mm in the tangential direction, and 10 mm in the longitudinal direction. The specimens were embedded in fresh Spurr low viscosity epoxy resin (Spurr 1969). The embedding

was performed in a flat mould with the wood specimen in the middle of the flat surface. The mould containing the wood samples and the epoxy resin was then placed in a vacuum oven. After being kept in a vacuum for a minimum of 12 h, the embedded samples were heated to 70 °C for 8 h until the resin cured. The resin-embedded sample was cut out from the mould and then mounted onto an ultra-microtome (American Optical Corp. USA). The transverse surface of the wood was leveled using a glass knife and then cut using a diamond knife for a smoother surface. Finally, the samples were conditioned for at least 24 h at 22 °C and 40% relative humidity in the nanoindenter laboratory.

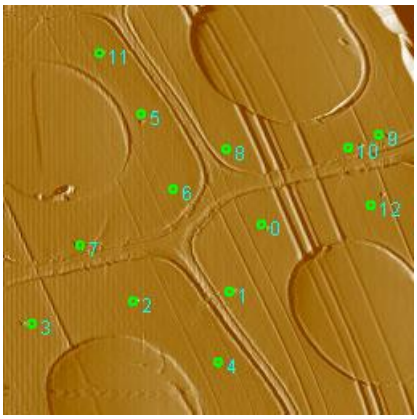

Fig. 1. Indent sites on compression wood

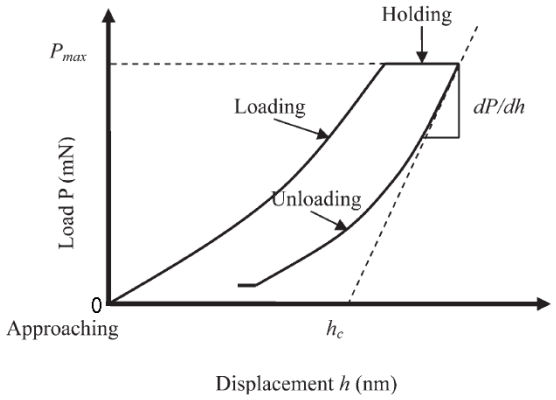

Fig. 2. Nanoindent load-displacement curve

The sample was directly placed into a specially designed holder and then fixed on a motorized sample stage by magnetic force. A nanoindenter (Hysitron Inc. USA) equipped with a three-sided pyramid diamond Berkovich type indenter tip was chosen to conduct the nanoindentation tests. The peak load and loading-unloading rate were 150 μN and 30 μN/s, respectively. The load holding time was 5 s between loading and unloading segments to allow for thermal drift corrections. The indent depth was about 120 nm under these conditions. The target region was scanned before and after each experiment using the instrument video system to determine the actual positions and quality of the indentations (Fig. 1).

The indents were made near the middle of the cell wall S_2 layer and distributed within the radial and tangential walls so as to reduce the error caused by the angle of tip. At least five tracheids from latewood were examined for each annual ring, and at least 50 measurements were taken for each of the rings investigated in this study.

A typical load-displacement curve of a nanoindent is shown in Fig. 2. It was found that both elastic and plastic deformation occurred during loading and only the elastic part of the displacement was recovered when unloading. Nanoindentation hardness (H) is defined by the following equation,

$$H = P_{max}/A \quad (1)$$

where P_{max} is the peak load and A is the projected contact area that is calculated from the empirical formula 24.5 hc^2, where hc is the contact depth of the indent.

The sample modulus (E_s) can be calculated as follows,

$$E_s = (1 - \nu_s^2)\left(\frac{1}{E_r} - \frac{1 - \nu_i^2}{E_i}\right) \quad (2)$$

where E_i and ν_i are respectively the elastic modulus and Poisson ratio of the tips. For diamond tips, E_i is 1141 GPa, and ν_i is 0.07. ν_s is the Poisson ratio of samples. It should be pointed out that the E_s and E_r are almost identical for soft materials like bamboo and wood, which eliminates the need to obtain the Poisson ratio of the samples. E_r is called the reduced elastic modulus, and can be obtained from the following equation,

$$E_r = S\sqrt{\pi} / A / 2\beta \quad (3)$$

where β is a constant that depends on the geometry of the indenter (β = 1.034 for a Berkovich indenter) and S is the initial slope of the unloading curve (this slope is the elastic contact stiffness). In these tests, a range covering 70 to 90% of the unloading curve was chosen for calculating $S(d_p/d_h)$.

RESULTS AND DISCUSSION

Nanoindentation is a very effective method for investigating the mechanical properties of the cell wall S_2 layer (Yu *et al.* 2012). Compared to other methods, there is no need for any chemical pretreatment of the sample, and the measured values are very consistent with a variation coefficient of about 10% for MOE and less than 8% for hardness.

Modulus of Elasticity (MOE)

The MOE of the cell wall S_2 layer of opposite wood and compression wood are summarized in Tables 1 and 2. The average MOE of opposite wood is slightly higher at 17.71 GPa than that of compression wood (16.65 GPa). A similar increase of the Young's modulus of opposite wood was found by Gindl (2002). The MOE has been shown to have a highly negative correlation to the value of MFA (Cave 1968, 1969; Page *et al.* 1977; Wu *et al.* 2009). As can be seen from Tables 1 and 2, compression wood had an average MFA 10° greater than opposite wood. However, the average MOE of compression wood was a little lower than opposite wood. When making nanoindentation measurements, the MOE is determined from the press-in mode of tip, which does not give the same results as measurements taken in tensile mode. Thus the MFA has a smaller influence on indentation than tension results. Furthermore, other factors must also play a role. Gillis and Mark (1973) showed that the MOE of cellulosic fibers with a MFA exceeding 25° was insensitive to the properties of the cellulose. Instead, it depended largely on the other characteristics. The compression wood had thick cell wall S_2 and S_1 layers, which could

provide support when the tip was pressed in and pulled out. Schniewind (1962) points out that a high concentration of lignin in the secondary wall could lead to a higher lateral stability of the microfibrils. Hence, the special structure of compression wood, characterized by thick cell wall S_2 and S_1 layers and a high content of lignin, reduces the difference in average MOE resulting from MFA.

Table 1. Cell Wall S_2 Layer Mechanical Properties and MFA of Opposite Wood

	O2	O4	O6	O9	O15	O24
MOE (GPa)	17.34	15.75	16.66	17.16	18.90	20.46
Hardness (GPa)	0.5317	0.4766	0.4881	0.4423	0.4605	0.5216
MFA (°)	22.54	26.01	17.02	14.58	11.53	12.57

Table 2. Cell Wall S_2 Layer Mechanical Properties and MFA of Compression Wood

	C2	C4	C6	C9	C15	C24
MOE (GPa)	14.72	15.54	15.89	17.16	19.05	17.53
Hardness (GPa)	0.4483	0.4084	0.4256	0.4863	0.4807	0.5073
MFA (°)	32.34	33.28	29.00	19.91	25.18	25.19

Generally, the MOE showed an increasing tendency with an increase of annual ring age for both compression wood and opposite wood (Tables 1 and 2), especially from annual ring 6, which was in good agreement with the adaptability growing of structure and function of trees (Meinzer *et al.* 2011). However, the tendency of MFA with annual ring age was to decrease (Fig. 3) (Cave and Walker 1994).

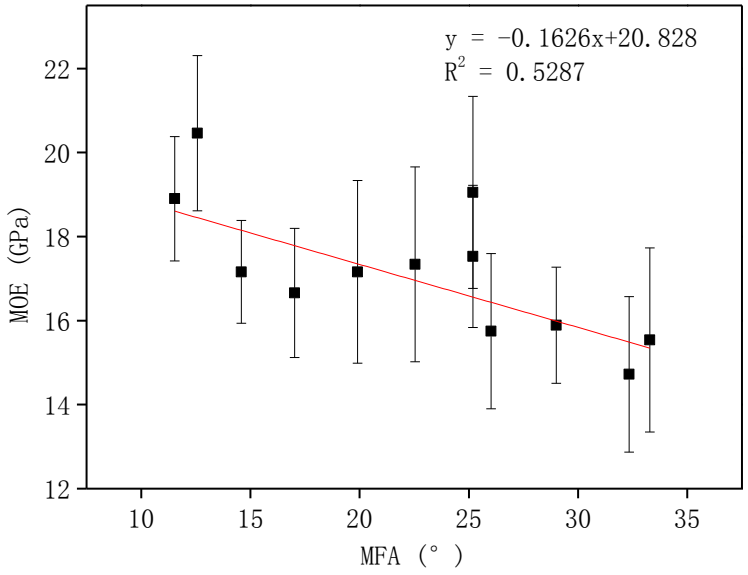

Fig. 3. Variation of MOE with MFA for all tested wood samples

MFA is known as a particularly important factor for mechanical properties of wood (Burgert *et al.* 2004; Tze *et al.* 2007; Wu *et al.* 2009), and a decrease in MFA would result in an increase of MOE in both opposite wood and compression wood. Linear regression analysis (Fig. 3) shows a weak relationship between MFA and MOE ($R^2 = 0.5287$) that also indicates that the cell wall MOE is influenced by multiple factors, such as entrained epoxy resin, as well as cell wall structure and components.

For samples taken from the same annual ring, the average value of MOE of opposite wood was higher than that of compression wood, which can be explained by the difference in MFA. However, the difference in the corresponding annual rings of MOE was small (about 1 GPa). The press-in mode of nanoindentation could be an important factor. Considering the special structure of the cell walls of compression wood, for example, the lack of an S_3 layer and the presence of large helical cavities in the S_2 layer, means that the embedding Spurr epoxy resin can easily enter these large helical cavities. The presence of the epoxy resin reinforces the cell walls of the compression wood and reduces the effect of MFA on the mechanical properties of the cell wall. Furthermore, as previously mentioned, the thick cell wall S_2 and S_1 layers and their high content of lignin may also have reduced the difference. Hence, it seems reasonable that there should be a somewhat low correlation coefficient between MFA and MOE in Fig. 3. The MOE of the second annual ring was high (17.34 GPa), which may have been caused by entrained resin in the samples.

Hardness

The average cell wall hardness of opposite wood and compression wood were not significantly different (0.4868 GPa and 0.4594 GPa). This similarity is supported by the results of Gindl *et al.* (2004) and Yu *et al.* (2007). Yu *et al.* (2007) indicated that the MFA does not greatly influence hardness. So when the MFA reaches a certain critical value, the composition and packing density of the cell walls will act as the determinant of cell-wall hardness (Yu *et al.* 2007). Gindl *et al.* (2004) also indicated that the indentation hardness was governed by the matrix at the macro level, for example, lignin content.

As is shown in Tables 1 and 2, there was a increasing trend of variation in cell wall hardness from annual ring 9 of opposite wood and compression wood, which could also be supported by Meinzer *et al.*'s theory of adaptability growing (2011). In the same annual ring, it appeared that there was no consistent rule for the average values of hardness of opposite and compression wood. This also indicates that MFA has little influence on the cell wall hardness of opposite wood and compression wood. According to macro-scale mechanical measurements, compression wood has a high lignin content and density, which results in high hardness level in bulk wood samples. However, Wu *et al.* (2009) also did not observe any distinct difference while making observations at the nanometer level. It was proposed that the special structure of the cell wall of compression wood would be the main factors rather than lignin content on cell wall hardness.

Mechanical Property Variation within an Annual Ring

Figure 4 shows the average MOE and standard deviation of cell wall of early, transition, and late wood within the 24th annual ring of Masson pine opposite wood. The average MOE of the cell wall of early (19.95 GPa), transition (19.95 GPa), and late

(21.08 GPa) wood were not significantly different. Variation of MOE is highly dependent on changes in MFA (Cave 1968, 1969; Page *et al.* 1977). Since there is little variation of MFA in mature wood annual rings (Eder *et al.* 2009), it is reasonable to assume that the difference of cell wall MOE should also be insignificant. Eder *et al.* (2009) also reported that the mechanical properties of spruce single fibers were similar throughout an annual ring in transition wood, which also supports the results in this study.

As Fig. 4 shows, the distribution range of the standard deviation of cell wall MOE of early wood was larger than that of late wood and transition wood, which was due to the location of the nanoindentations and the thickness of cell wall.

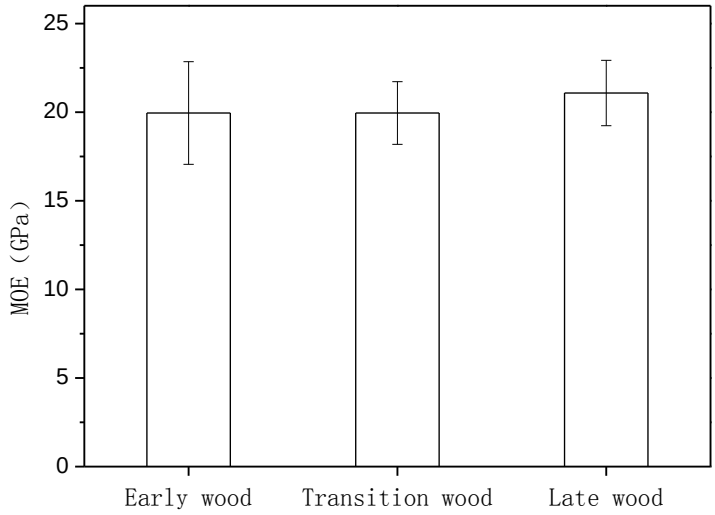

Fig. 4. Cell wall MOEs and standard deviations of early, late, and transition wood within the 24th annual ring of Masson Pine opposite wood (error bars represent standard deviation).

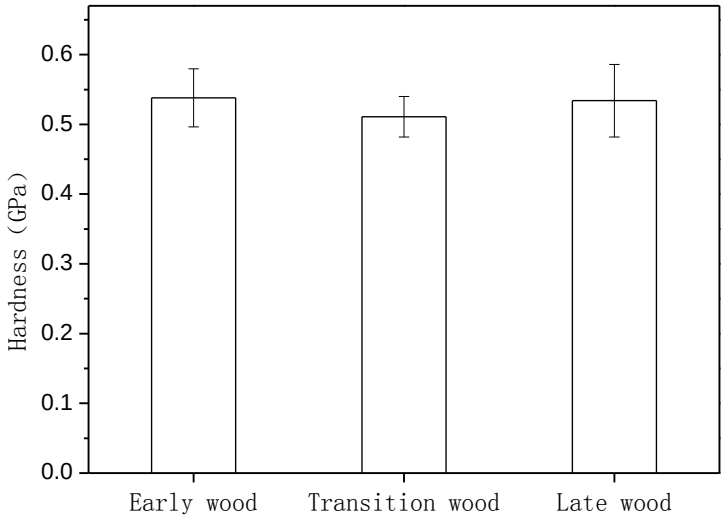

Fig. 5. Cell wall hardness and standard deviation of early, late, and transition wood within the 24th annual ring of Masson Pine opposite wood (error bars represent standard deviation).

Generally, the thickness of the cell wall was different among early, transition, and late wood in the same annual ring. The early wood had a thinner cell wall than that of late wood and transition wood. Thus, the thinner the cell walls, the higher the possibility of dislocation of the indentation tip. The MOE was slightly higher when the location of tip insertion neared the fringe of the cell wall, but a little lower when it was near the edge of the cell cavity. Therefore, for early wood, the MOE value was less repeatable than for other woods. The distribution range of standard deviations of cell wall MOE was also large.

For hardness, as with measurements of MOE, no difference existed among early, transition, and late wood in the same annual ring (Fig. 5). However, the standard deviations of cell wall hardness did not match that of cell wall MOE. According to Yu *et al.* (2007) and Gindl *et al.* (2004), indentation hardness is governed by the characteristics of the matrix. Since the cell wall hardnesses were similar in early, transition, and late wood of the same annual ring, it was reasonable to infer that the matrix properties in a mature annual ring were also similar.

CONCLUSIONS

Nanoindentation is a very powerful method for investigating the mechanical properties of the cell wall S_2 layer of compression wood at the nanoscale. The average values of the hardness and MOE of opposite wood were slightly higher than those of compression wood. The MOE increased with increasing annual ring age for both compression and opposite wood, which is mostly due to a decreasing trend in MFA. An increasing trend was also observed for hardness form annual ring 9. In opposite and compression wood taken from the same annual ring, the differences in average values of modulus of elasticity and hardness were all insignificant. The lack of difference was explained by the change in MFA, the press-in mode of nanoindentation, and the special structure of compression wood. For early, transition, and late wood within the same opposite wood annual ring, the MOE and the hardness were both very similar. It is reasonable to infer that the thickness of the cell wall S_2 layer has no effect on the nanoindentation testing values in a mature annual ring.

ACKNOWLEDGMENTS

This work was financially supported by projects from the National Natural Science Key Foundation of China (Grant No. 30730076) and the USDA Wood Utilization Research Grant.

REFERENCES CITED

Burgert, I., Fruhmann, K., Keckes, J., Fratzl, P., and Stanzl-Tschegg, S. (2004). "Structure function relationships of four compression wood types: Micromechanical properties at the tissue and fibre level," *Trees* 18(4), 480-485.

Cave, I. D. (1966). "Theory of X-ray measurement of microfibril angle in wood," *Forest Prod. J.* 16, 37-42.

Cave, I. D. (1968). "The anisotropic elasticity of the plant cell wall," *Wood Sci. Technol*. 2(4), 268-278.

Cave, I. D., and Walker, J. C. F. (1994). "Stiffness of wood in fast-grown plantation softwoods: The influence of microfibril angle," *Forest Prod. J.* 44, 43-48.

Eder, M., Jungnikl, K., and Burgert, I. (2009). "A close-up view of wood structure and properties across a growth ring of Norway spruce (*Picea abies* [L] Karst.)," *Trees* 23, 79-84.

Gillis, P. P., and Mark, R. E. (1973). "Analysis of shrinkage, swelling and twisting of pulp fibers," *Cellul. Chem. Technol*. 7, 209-234.

Gindl, W. (2002). "Comparing mechanical properties of normal and compression wood in Norway spruce: The Role of lignin in compression parallel to the grain," *Holzforschung* 56, 395-401.

Gindl, W., Gupta, H. S., Schöberl, T., Lichtenegger, H. C., and Fratzl, P. (2004). "Mechanical properties of spruce wood cell walls by nanoindentation," *Appl. Phys. A* 79, 2069-2073.

Konnerth, J., Gierlinger, N., Keckes, J., and Gindl, W. (2009). "Actual versus apparent within cell wall variability of nanoindentation results from wood cell walls related to cellulose microfibril angle," *J. Mater. Sci*. 44, 4399-4406.

Meinzer, F. C., Lachenbruch, B., and Dawson, T. E. (2011). *Size and Age-related Changes in Tree Structure and Function*, Springer, Dordrecht, 510 pp.

Page, D. H., EI-Hosseiny, F., Winkler, K., and Lancaster, A. P. S. (1977). "Elastic modulus of single wood pulp fibers," *Tappi* 60(4), 114-117.

Schniewind, A. P. (1962). "Mechanical behavior of wood in the light of its anatomic structure," In: Schniewind, A. P. (ed.), *The Mechanical Behavior of Wood*, Conf. Univ. CA, Berkeley, 136-146.

Spurr, A. R. (1969). "A low-viscosity epoxy resin embedding medium for electron microscope," *J. Ultrastruct. Res*. 26, 31-43.

Timell, T. E. (1987). *Compression Wood in Gymnosperms*, Vol. 1, Springer Verlag, Heidelberg.

Tze, W. T., Wang, S., Rials, T. G., Pharr, G. M., and Kelley, S. S. (2007). "Nanoindentation of wood cell wall: Continuous stiffness and hardness measurement," *Comp. A–Appl. Sci. Manufact*. 38, 945-953.

Wu, Y., Wang, S., Zhou, D., Xing, C., Zhang, Y., and Cai, Z. (2010). "Evaluation of elastic modulus and hardness of crop stalks cell walls by nano-indentation," *Bioresour. Technol.* 101, 2867-2871.

Yu, Y., Fei, B., Wang, H., and Tian, G. (2012). "Longitudinal mechanical properties of cell wall of Masson pine (*Pinus massoniana* Lamb) as related to moisture content: A nanoindentation study," *Holzforschung* 65(1), 121-126.

Yu, Y., Fei, B., Zhang, B., and Yu, X. (2007). "Cell wall mechanical properties of Bamboo investigated by in-situ imaging nanoindentation," *Wood Fiber Sci.* 39(4), 527-535.

Article submitted: March 22, 2012; Peer review completed: May 19, 2012; Revised version received and accepted: May 23, 2012; Published: May 25, 2012.